

# Is perpendicular magnetic anisotropy essential to all-optical ultrafast spin reversal in ferromagnets?

G. P. Zhang

*Department of Physics, Indiana State University, Terre Haute, IN 47809, USA*

Y. H. Bai

*Office of Information Technology, Indiana State University, Terre Haute, IN 47809, USA*

Thomas F. George

*Office of the Chancellor and Center for Nanoscience*

*Departments of Chemistry & Biochemistry and Physics & Astronomy*

*University of Missouri-St. Louis, St. Louis, MO 63121, USA*

(Dated: October 22, 2018)

## Abstract

All-optical spin reversal presents a new opportunity for spin manipulations, free of a magnetic field. Most of all-optical-spin-reversal ferromagnets are found to have a perpendicular magnetic anisotropy (PMA), but it has been unknown whether PMA is necessary for the spin reversal. Here we theoretically investigate magnetic thin films with either PMA or in-plane magnetic anisotropy (IMA). Our results show that the spin reversal in IMA systems is possible, but only with a longer laser pulse and within a narrow laser parameter region. The spin reversal does not show a strong helicity dependence where the left- and right-circularly polarized light lead to the identical results. By contrast, the spin reversal in PMA systems is robust, provided both the spin angular momentum and laser field are strong enough while the magnetic anisotropy itself is not too strong. This explains why experimentally the majority of all-optical spin-reversal samples are found to have strong PMA and why spins in Fe nanoparticles only cant out of plane. It is the laser-induced spin-orbit torque that plays a key role in the spin reversal. Surprisingly, the same spin-orbit torque results in laser-induced spin rectification in spin-mixed configuration, a prediction that can be tested experimentally. Our results clearly point out that PMA is essential to the spin reversal, though there is an opportunity for in-plane spin reversal.

## I. INTRODUCTION

Laser-controlled spin dynamics in ferromagnets started with the pioneering work by Beaurepaire and coworkers [1], who found that an ultrafast laser pulse is capable of demagnetizing a nickel thin film within 1 ps. This opens a new frontier in magnetism that has never been seen before. Earlier studies heavily concentrated on how such an ultrashort demagnetization occurs, a still hotly debated topic even today [2–7]. Technological implications of this discovery was recognized in the beginning, and soon investigations of the exchange-coupled structure [8], a prime example in spintronics, started. The results were very interesting, but not surprising.

A decade earlier, Gau [9] reviewed several important materials used in magneto-optical recording (MO) and laid out the ideal structure-property relationship for technological applications. Amorphous rare-earth transition metals were first reported in 1973 by the IBM group [10], where  $(\text{Tb,Gd})_x(\text{Fe,Co})_{1-x}$  ferrimagnetic thin films with  $0.2 \leq x \leq 0.3$  represent the archetype material for MO. These films have a perpendicular magnetic anisotropy (PMA) and two spin sublattices. The sublattices allow the compensation temperature, where two sublattice spins cancel each other, to be tuned toward room temperature [9]. The writing is done through an AlGaAs semiconductor laser and a magnetic field.

In 2007, using GdFeCo, Stanciu *et al.* [11] reported that the writing is possible even with a single laser pulse but without a magnetic field. The helicity determines how the spin is reversed [12, 13]. Left-circularly polarized light switches spins from down to up, while right-circularly polarized light does the opposite. This is commonly called all-optical helicity-dependent spin switching, or AOHDs. A group of new materials has emerged lately [14, 15]. Of particular interest are ferromagnetic CoPt ultrathin films. They only have a single spin lattice since Pt sites have a much weaker spin moment. The films have only 1-2 monolayers, and thicker ones do not show AOHDs. What is surprising is that these samples also have PMA. This is not limited to CoPt. John and coworkers discovered that in FePt nanoparticles with PMA, magnetization switching is possible [16]. Different from CoPt and FePt, iron nanoparticles have an in-plane magnetic anisotropy (IMA). Recently, Ren and coworkers [17] found that upon ultrafast laser excitation, in-plane spins in iron nanoparticles only cant out of the plane of their sample and are not switched over. This indicates that the initial spin configuration is likely to have an important impact on how spins react to laser

excitation, a theme also revealed in dysprosium [18]. Is PMA essential to all-optical spin switching (AOS)? To answer this, we believe that a theoretical investigation is imperative.

In this paper, we present a theoretical investigation to establish the intricate connection between the spin configurations (PMA and IMA) and switchability of the spins on the shortest possible time scale. We employ our newly developed model to directly compute the spin evolution in the time domain. We demonstrate theoretically that PMA has an unparalleled advantage over IMA to switch spins. Its switching window is much broader, and the spin precesses orderly. The switching is robust. By contrast, the switching in IMA systems is often subject to chaotic spin precession. If the laser pulse is too short, the spin reversal does not occur. Only when we increase the laser pulse duration to 120 fs do we find a narrow region in which the spin does reverse. The key player is the spin-orbit torque. At the optimal laser field amplitude, the in-plane torque (for IMA) is larger than those along the other directions, so switching occurs. If we mix PMA with IMA, we find that there is no switching, but quite surprisingly, the spins in each layer, after the laser excitation, proceed in harmony, a prediction that can be verified in experiments. Our results clarify the role of spin configuration in spin reversal and should have some important implications for the future research in AOS.

The rest of the paper is arranged as follows. In Sec. II present our spin reversal theory. Section III is devoted to our main results and discussions. We start with the perpendicular magnetic anisotropy and then move on to the in-plane magnetic anisotropy, followed by two investigations in the mixed spin configuration. Finally, we conclude this paper in Sec. IV.

## II. SPIN REVERSAL THEORY

Femtomagnetism [19] is not a traditional topic in magnetism. The traditional spin wave theory only describes spin dynamics under a magnetic or thermal field [20], not a laser field. Since the beginning of AOS, enormous efforts have been made to develop a reasonably simple theory to explain AOS, and over ten theories have been proposed [11, 21–32].

Recently, when we investigated the magneto-optical Kerr effect [31, 33], we unexpectedly found a rather simple method. This method only captures the initial steps of the spin reversal, thus complementing other methods [11, 21–29] very well. While the details of our method have been published [31], here we briefly review some basic ideas behind our theory.

Our method starts from the traditional model, very popular in optics and nonlinear optics, where the electron is placed in a harmonic potential  $m\Omega^2\mathbf{r}^2/2$  with frequency  $\Omega$  and interacts with the laser field through the dipole term,  $-e\mathbf{E}(t) \cdot \mathbf{r}$ , where  $-e$  is the electron charge,  $\mathbf{E}(t)$  is the electric field of the laser pulse, and  $\mathbf{r}$  is the position of the electron. However, the traditional model has no spin, so the interaction between the laser and spin is missing. To overcome this deficiency, the magneto-optical theory includes a magnetic field,  $\mathbf{B}_{ext}$ , besides the electric field. The effect on the magnetic property of the system comes from the Lorentz interaction, but spin is still missing. A major breakthrough came when we realized that we can amend the spin-orbit coupling (SOC)  $\lambda\mathbf{L} \cdot \mathbf{S}$  to the original Hamiltonian, where  $\lambda$  is the spin-orbit coupling,  $\mathbf{L}$  is the orbital angular momentum, and  $\mathbf{S}$  is the spin angular momentum. The electron experiences an additional force from SOC. The orbital angular momentum is computed from the position and momentum of the electron, i.e.,  $\mathbf{r} \times \mathbf{p}$ . Then the Hamiltonian for a single electron at site  $i$  is [30, 33]

$$H_i(t) = \frac{\mathbf{p}_i^2}{2m} + \frac{1}{2}m\Omega^2\mathbf{r}_i^2 + \lambda\mathbf{L}_i \cdot \mathbf{S}_i - e\mathbf{E}(t) \cdot \mathbf{r}_i, \quad (1)$$

where the first and second terms are the kinetic and potential energy terms, respectively, and the last term is the interaction between the laser electric field  $\mathbf{E}(t)$  and the system. This Hamiltonian is not different from those used in nonlinear optics [34], except for the spin-orbit term. This Hamiltonian is also similar to the  $t - J$  model [35], so the itinerant nature of the electron is captured. But the  $t - J$  model can not be used to simulate AOS, since it has no orbital angular momentum, at least in the original Hamiltonian where the orbital character is hidden. What we did here is to essentially expand the spatial dimension of the model into the spin space. This builds a crucial link between the laser and the spin system [33]. Despite this complication, being able to treat both spin and spatial spaces opens a new path to simulate the spin dynamics in a real time domain and permits us to attack the most difficult issue at the hard core of AOS.

If we fix the spin  $\mathbf{S}$ , then we recover the previous magneto-optical results [33]. If we allow the spin to change, a source term, namely a spin-orbit torque, appears

$$\left(\frac{d\mathbf{S}_i}{dt}\right)_{soc} = \lambda(\mathbf{L}_i \times \mathbf{S}_i), \quad (2)$$

which describes how the spin changes at site  $i$ . Our previous work demonstrated varieties of possible switching within this single-site model. We avoid electron and spin temperatures on

a time scale and an effective magnetic field [21]. This presents a more consistent formalism for spin reversal at the shortest possible time scale. For spin dynamics on a long time scale, one may refer to prior studies [21–29].

Another important contribution is from the exchange interaction. Ramsay *et al.* [36] showed that in GaMnAsP photocarrier spin exerts a spin-transfer torque on the magnetization via the exchange interaction. To take into account the magnetic interaction and go beyond a single-site approximation, we include the Heisenberg exchange interaction term for site  $i$

$$H_i^{ex} = - \sum_{j(i)} J_{ij} \mathbf{S}_i \cdot \mathbf{S}_j, \quad (3)$$

where the summation is over the nearest-neighbor site  $j$  of spin  $\mathbf{S}_i$ .  $J_{ij}$  is the exchange interaction between sites  $i$  and  $j$ , and can be changed to simulate either ferromagnetic or antiferromagnetic ordering. This term induces an exchange torque,

$$\left( \frac{d\mathbf{S}_i}{dt} \right)_{ex} = \sum_{j(i)} J_{ij} \mathbf{S}_i \times \mathbf{S}_j. \quad (4)$$

We also consider adding a magnetic anisotropy term  $H_i^{\text{anis}} = -d(S_{z,i})^2$ , where  $d$  is the anisotropy constant. We find that for  $J_{ij} = 1$  eV, if  $d$  is on the order of  $10^{-5}$  eV, there is no major effect on our results within a few hundred femtoseconds. But if  $d$  is too strong,  $10^{-3}$ - $10^{-2}$  eV, the transverse components ( $S_x$  and  $S_y$ ) start to interfere with the longitudinal component ( $S_z$ ), so the spin switching becomes difficult. This happens to the in-plane anisotropy case as well. In our calculation, we do not include the dipolar interaction since it is rather weak and only acts on a much longer time scale. Our final Hamiltonian contains the Heisenberg exchange term and the single site Hamiltonian [37, 38]

$$H = \sum_i (H_i(t) + H_i^{ex}), \quad (5)$$

where the summation is over all the sites in the system. To compute the spin dynamics, we numerically solve the Heisenberg equation of motion for the spin operator  $\mathbf{S}$  [30],  $i\hbar\dot{\mathbf{S}} = [\mathbf{S}, H]$ , where  $\mathbf{S}$  is an operator and  $H$  is the total Hamiltonian of the system (Eq. 5). We employ the variable-order and variable steps Adams method [39] to solve the differential equation. The tolerance of calculation is set at  $5 \times 10^{-13}$  for over 6000 differential equations.

### III. RESULTS AND DISCUSSIONS

Our system consists of four monolayers along the  $z$  direction. There are 41 lattice sites along the  $x$  and  $y$  directions, respectively. This forms a simple cubic lattice structure. There are over 6400 spins in our system. We have confirmed that using an even larger number of spins has little effect on our results. Three types of spin configurations are considered: (a) perpendicular magnetic anisotropy, (b) in-plane magnetic anisotropy and (c) mixed anisotropy (see Fig. 1). A circularly polarized light coming down along the  $-z$  axis with a penetration depth of 40 lattice sites. The field itself [31, 33] is

$$\mathbf{E}(t) = A_0 e^{-t^2/\tau^2} (\mp \sin(\omega t) \hat{x} + \cos(\omega t) \hat{y}), \quad (6)$$

where  $A_0$  is the laser field amplitude,  $\omega$  is the carrier frequency,  $\tau$  is the laser pulse duration, and  $\hat{x}$  and  $\hat{y}$  are the unit vectors along the  $x$  and  $y$  directions, respectively.  $\mp$  in the equation refers to the left- (right-)circularly polarized light. Our exchange interaction is  $J = 1 \text{ eV}/\hbar^2$ , and the spin-orbit coupling is  $\lambda = 0.06 \text{ eV}/\hbar^2$ , typical for transition metals [20].

#### A. Perpendicular magnetic anisotropy

We align all the spins along the  $-z$  axis and couple them ferromagnetically, with the initial value of  $-1\hbar$ . The laser light impinges along the  $-z$  axis. Each layer is exposed with a different laser intensity. To start with, we use left-circularly polarized light with duration of 60 fs. The laser photon energy is  $\hbar\omega = \hbar\Omega = 1.6 \text{ eV}$ . There is no magnetic field in our simulation. Since we have 6400 spins, we decide to compute the layer-averaged spin and also monitor each spin evolution by sampling them individually. Figure 2(a) shows the layer-averaged spin as a function of time upon laser excitation for three components of the spin. The solid line is the  $z$  component. We see that it is reversed successfully from  $-1\hbar$  to  $0.75\hbar$ . This is consistent with our earlier calculation [30]. We do not have full spin reversal because our current spin angular momentum is still too low [30].  $S_x$  and  $S_y$  are zero in the beginning, but reach around  $-0.5\hbar$ . Spin oscillation is clearly visible for each component. For this reason, we compute the maximum and minimum for each component in Fig. 2(b). Importantly, not all the laser field amplitudes are capable of switching the spins. Figure 2(b) shows the layer-averaged spins as a function of laser field amplitude. We compute the maximum and minimum spins for each component after 300 fs (from when the laser peaks

at 0 fs). For PMA, the oscillation amplitude is small (compare the solid and dotted lines for  $S_x$ ,  $S_y$  and  $S_z$ ). We see that when the laser field amplitude is small, there is no spin reversal. But when the field increases,  $S_z$  increases sharply, while  $S_y$  decreases to a negative value. This change is typical [31] since the laser-induced spin-orbit torque that is needed to reverse the spin has to be positive along the  $z$  axis, so the  $S_z$  changes signs. For a field amplitude that is slightly larger than  $0.01 \text{ V/\AA}$ , the spin cants along the  $y$  axis. A transition occurs when the laser field amplitude is close to  $0.0165 \text{ V/\AA}$  and when the spin is reversed along  $+z$ . The subtle crossing between  $S_x$  and  $S_y$  signals the coming of the optimal reversal field. After this optimal value, the spin cants along the  $-x$  axis.

One of our important findings for PMA is that it shows a strong helicity-dependent switching. The lower line at the bottom of Fig. 2(b) plots the results with right-circularly polarized light. We see that it can not reverse the spin in the entire amplitude region. Here we only show the  $z$  component of the spins in the first layer, since the other components are too small to show. The huge difference between the left- and right-circularly polarized light is mainly due to the orbital angular momentum difference as noticed before [31].

## B. In-plane magnetic anisotropy

A naive guess for the in-plane magnetic anisotropy would be similar to PMA. However, quantum mechanically, IMA has the spin quantization along the  $x$  axis. Because the optical selection rule ( $\Delta l = \pm 1$ ,  $\Delta m_l = 0, \pm 1$  with  $l$  and  $m_l$ , respectively, being orbital and magnetic orbital angular momentum quantum numbers) is spatially relative to the spin quantization, the left- and right-circularly polarized light become equivalent to the spin. Such a convoluted relation is difficult to include if one uses a heat pulse in place of a true laser field. Our scheme shows the true power to simulate spin dynamics. In Fig. 2(c) we present a representative result for the spin precession. The laser field amplitude is chosen to be  $0.02 \text{ V/\AA}$ . We find that regardless of how strong or weak the laser field is, the switching is not observed. For a weak laser pulse, the spin oscillates with a smaller amplitude. For a stronger laser, the oscillation dominates the entire dynamics with a shorter period. Therefore, the maximum and minimum spins differ a lot (see Fig. 2(d)). To be sure that we do not miss the major portion of the laser parameter space, we extend the laser field amplitude all the way up to  $0.08 \text{ V/\AA}$ , and we do not find a case where the spin is reversed with duration  $\tau = 60 \text{ fs}$ . No

spin reversal is found, and no helicity dependence is noted.

From the huge oscillation in the spin in Fig. 2(d), we notice something unusual. The maximum spin can reach  $0.5 \hbar$  for the field amplitude below  $0.05 \text{V}/\text{\AA}$ , but its minimum is just too negative. Considering the laser peak around 0 fs, the spin appears to overshoot (see Fig. 2(c)). This is always the case with an ultrashort pulse, where the coherence lasts very long [40]. We wonder whether a longer pulse can suppress such a rapid oscillation. We increase the pulse duration to 120 fs. To our surprise, although the entire amplitude dependence does not change much, a window of opportunity appears. If one compares Fig. 3(a) with Fig. 2(d), the minimum spin increases overall, so the oscillatory amplitude drops. Because of the longer laser pulse duration, the relative field amplitude that yields the same change is also reduced. Around  $0.015 \text{ V}/\text{\AA}$ , the first optimal condition appears. Figure 3(b) shows the layer-averaged spin precession as a function of time. In the beginning, the spin is along the  $-x$  axis, and upon laser excitation, it tilts within the  $xy$  plane. The  $y$  component is comparable to the  $x$  component of about  $0.7 \hbar$ . In the middle of the lower panel of Fig. 3, we sketch the initial and final spins to show how the spin reversal is partially accomplished.

To understand how the switching occurs, we need to look at the spin-orbit torque upon laser excitation for each component of the spin. Figure 3(c) shows that in general the spin-orbit torque  $\tau_{soc}$  for each component is similar, but with one crucial exception:  $\tau_y$  and  $\tau_z$  peak much earlier. This explains why  $S_y$  and  $S_z$  rise earlier and more quickly. This is fully expected, since in the beginning the spins are zero along these two directions, and the torque is a product of the spin along the other direction with the orbital angular momentum. The challenge to understand the spin reversal is that these three components obey the mutual permutation relation  $[S_x, S_y] = i\hbar S_z$  [37]. If one of these components is zero and stays at zero, the spin reversal is not possible. Thus, normally the linear spin reversal proposed by Stanciu *et al.* [11] does not occur. This is reflected in our simulation. Once  $S_y$  and  $S_z$  are different from zero,  $S_x$  can be switched. Since the torques from the laser and the exchange interaction are weak in the ferromagnetic configuration [31], the key driver to reverse  $S_x$  is the spin-orbit torque. Figure 3(c) further shows that  $\tau_x$  (solid line) is smaller than  $\tau_y$  (dotted line) and  $\tau_z$  (dashed line), except around 0 fs when the laser peaks. Its magnitude surpasses both  $\tau_y$  and  $\tau_z$ . It is in this narrow temporal window that  $S_x$  reverses its direction, after which  $\tau_x$  decreases. Such a decrease is necessary, since otherwise the switched spin would undergo a strong oscillation.



In PMA, the helicity dependence is very strong, but in IMA the helicity dependence is absent due to the selection rule discussed above. This is also confirmed numerically. In summary, we assert that AOS in IMA is much harder to obtain than PMA. This explains the crucial experimental observation as to why most AOS ferromagnets have a perpendicular magnetic anisotropy.

### C. Laser-guided spin mode rectification

So far, our spin configurations are very pure – either perpendicular magnetic anisotropy or in-plane magnetic anisotropy. Magnetic orderings can be a mix of several different configurations and may contain different domains. Without considering all the possible spin configurations and without changing the system size, we examine what happens to the spin switching if the first layer of spins has PMA but the rest IMA (see Fig. 1(c)). From Eq. (4), we see that such a configuration will induce a strong exchange torque, so the spin precession is highly nonlinear. One would expect that the laser has no big effect on the spin precession because the precession is already chaotic. However, to our surprise, this does not happen.

We use a 60-fs laser pulse with left-circularly polarized light and employ an extremely weak laser of  $A_0 = 0.001\text{V}/\text{\AA}$ , so as to perturb the system gently. We start with a field-free case. Figure 4(a) shows  $S_z$  on layer 1 changing with time. Other components oscillate similarly and strongly overlap with  $S_z$ . Also in other layers, the spins are similar, so we do not show them. This is fully expected as discussed above. The period of the oscillation is determined by both the exchange interaction  $J_{ij}$  and the spin angular momentum, together with the spin-orbit coupling [41]. Figure 4(b) shows the same spin component as Fig. 4(a) but in the presence of a laser pulse. We see that the fluctuation in the original field-free dynamics is strongly suppressed. The amplitude of the spin oscillation is reduced from  $2\hbar$  to less than  $0.25\hbar$ . The spin is rectified according to the laser field. The laser pulse is shown in the inset of Fig. 4(b). Since left-circularly polarized light has nonzero  $x$  and  $y$  components, these components superimpose on top of each other in the inset. The horizontal line represents zero for the laser field. The field has duration of 60 fs, so its nonzero field extends from -300 fs to +300 fs.

Such spin rectification is not limited to the first layer. We find that all the layers have this feature. Figure 4(c) shows the  $x$  component of the layer-averaged spin in layer 2. On the top

is the spin without laser excitation, and the bottom is with laser excitation. The difference is very clear. We also use different laser parameters, and the results are the same. This unexpected result requires an experimental confirmation. Microscopically, we find that the laser acts like a pivot that steers the spin along one particular direction. This is consistent with our earlier finding that the laser-induced spin-orbit torque is significantly larger than the energy barrier to alter the spin configuration [30].

To have some qualitative feeling as to how the spins change across different layers, in Table I we show the initial and final layer-averaged spins. A pattern emerges. Although the initial spins are not in parallel, upon the laser excitation the spins in different layers congregate into the same orientation to reduce the exchange energy. Since there are three layers ferromagnetically coupled, the first layer with the original PMA bends its spins toward the other layers. Future experiments can test our prediction. Layered materials are popular in spintronics and spin-valve devices, where one essentially has a trilayer structure with a nonmagnetic spacer in between two layers. If the exchange coupling is strong between two ferromagnetic layers, even if the spin orientations at these two end layers are different, upon laser excitation, they can be guided into the same direction. We also test another case where two top layers have spin perpendicular anisotropy. As seen from the same table, the results are similar. This suggests that this laser-induced rectification is quite robust. We plan to investigate the helical configuration in the future. Experimentally, Ju *et al.* [8] in their first experiment did see the impact of the laser pulse on the exchange bias. An extension of their experiment should be able to verify our prediction.

After this work was finished, we noticed that Laliu *et al.* [42] experimentally investigated the same mechanism in noncollinear magnetic bilayers, where one layer has spin out of plane while the other layer spin is in plane, separated by a spacer layer. They showed that they could absorb or generate spin currents. This is consistent with an earlier study by Huisman *et al.* [43], where optical generation of spin currents was demonstrated in a 10-nm thick Co film deposited on a 2-nm Pt layer.

#### IV. CONCLUSION

We have investigated a hitherto open question as to whether the perpendicular magnetic anisotropy is essential to all-optical laser-induced spin reversal in ferromagnets. Our finding

is affirmative that PMA has a commanding advantage over IMA. AOS emerges, as both the laser field amplitude and the spin angular momentum are large enough. The spin does not show a strong oscillation, which is a big advantage for future applications. However, our finding does not exclude AOS in IMA. For a long laser pulse (120 fs), we find that there is a narrow region where a partial reversal is still possible. We predict that in a mixed spin configuration, a laser pulse can effectively rectify the spin evolution by suppressing spin frustration. We look forward to an experimental confirmation.

## ACKNOWLEDGMENTS

This work was solely supported by the U.S. Department of Energy under Contract No. DE-FG02-06ER46304. Part of the work was done on Indiana State University's quantum cluster and high-performance computers (obsidian and spin). The research used resources of the National Energy Research Scientific Computing Center, which is supported by the Office of Science of the U.S. Department of Energy under Contract No. DE-AC02-05CH11231.

- 
- [1] E. Beaurepaire, J. C. Merle, A. Daunois, and J.-Y. Bigot, Ultrafast spin dynamics in ferromagnetic nickel, *Phys. Rev. Lett.* **76**, 4250 (1996).
  - [2] B. Koopmans, G. Malinowski, F. Dalla Longa, D. Steiauf, M. Föhnle, T. Roth, M. Cinchetti, and M. Aeschlimann, Explaining the paradoxical diversity of ultrafast laser-induced demagnetization, *Nat. Mat.* **9**, 259 (2010).
  - [3] S. Mathias, C. La-O-Vorakiat, P. Grychtol, P. Granitzka, E. Turgut, J. M. Shaw, R. Adam, H. T. Nembach, M. E. Siemens, S. Eich, C. M. Schneider, T. J. Silva, M. Aeschlimann, M. M. Murnane, and H. C. Kapteyn, Probing the timescale of the exchange interaction in a ferromagnetic alloy, *PNAS* **109**, 4792 (2012).
  - [4] C. Stamm, T. Kachel, N. Pontius, R. Mitzner, T. Quast, K. Holldack, S. Khan, C. Lupulescu, E. F. Aziz, M. Wietstruk, H. A. Dürr, and W. Eberhardt, Femtosecond modification of electron localization and transfer of angular momentum in nickel, *Nat. Mat.* **6**, 740 (2007).
  - [5] C. La-O-Vorakiat, M. Siemens, M. M. Murnane, H. C. Kapteyn, S. Mathias, M. Aeschlimann, P. Grychtol, R. Adam, C. M. Schneider, J. M. Shaw, H. Nembach, and T. J. Silva, Ultrafast

- demagnetization dynamics at the M edges of magnetic elements observed using a tabletop high-harmonic soft x-ray source, *Phys. Rev. Lett.* **103**, 257402 (2009).
- [6] E. Turgut, C. La-o-vorakiat, J. M. Shaw, P. Grychtol, H. T. Nembach, D. Rudolf, R. Adam, M. Aeschlimann, C. M. Schneider, T. J. Silva, M. M. Murnane, H. C. Kapteyn, and S. Mathias, Controlling the competition between optically induced ultrafast spin-flip scattering and spin transport in magnetic multilayers, *Phys. Rev. Lett.* **110**, 197201 (2013).
- [7] E. Turgut, D. Zusin, D. Legut, K. Carva, R. Knut, J. M. Shaw, C. Chen, Z. Tao, H. T. Nembach, T. J. Silva, S. Mathias, M. Aeschlimann, P. M. Oppeneer, H. C. Kapteyn, M. M. Murnane, and P. Grychtol, Stoner versus Heisenberg: Ultrafast exchange reduction and magnon generation during laser-induced demagnetization, *Phys. Rev. B* **94**, 220408 (2016).
- [8] G. Ju, A. V. Nurmikko, R. F. C. Farrow, R. F. Marks, M. J. Carey, and B. A. Gurney, Ultrafast time resolved photoinduced magnetization rotation in a ferromagnetic/antiferromagnetic exchange coupled System, *Phys. Rev. Lett.* **92**, 3705 (1999).
- [9] J. S. Gau, Magneto-optical recording materials, *Mat. Sci. Eng.* **B3**, 371 (1989).
- [10] P. Chaudhari, J. J. Cuomo, and R. J. Gambino, Amorphous metallic films for magneto-optic applications, *Appl. Phys. Lett.* **22**, 337 (1973).
- [11] C. D. Stanciu, F. Hansteen, A. V. Kimel, A. Kirilyuk, A. Tsukamoto, A. Itoh, and Th. Rasing, All-optical magnetic recording with circularly polarized light, *Phys. Rev. Lett.* **99**, 047601 (2007).
- [12] M. S. El Hadri, P. Pirro, C.-H. Lambert, N. Bergeard, S. Petit-Watelot, M. Hehn, G. Malinowski, F. Montaigne, Y. Quessab, R. Medapalli, E. E. Fullerton, and S. Mangin, Electrical characterization of all-optical helicity-dependent switching in ferromagnetic Hall crosses, *Appl. Phys. Lett.* **108**, 092405 (2016).
- [13] G.-M. Choi, A. Schleife, and D. G. Cahill, Optical-helicity-driven magnetization dynamics in metallic ferromagnets, *Nat. Commun.* **8**, 15085 (2017).
- [14] C.-H. Lambert *et al.*, All-optical control of ferromagnetic thin films and nanostructures, *Science* **345**, 1337 (2014).
- [15] S. Mangin *et al.*, Engineered materials for all-optical helicity-dependent magnetic switching, *Nat. Mat.* **13**, 286 (2014).
- [16] R. John, M. Berritta, D. Hinzke, C. Müller, T. Santos, H. Ulrichs, P. Nieves, J. Walowski, R. Mondal, O. Chubykalo-Fesenko, J. McCord, P. M. Oppeneer, U. Nowak, and M. Münzenberg,

- Magnetization switching of FePt nanoparticle recording medium by femtosecond laser pulses, *Scientific Reports* **7**, 4114 (2017); also arXiv: 1606.08723 (2016).
- [17] Y. H. Ren, W. Lai, Z. Cevher, Y. Gong, and G. P. Zhang, Experimental demonstration of 55-fs spin canting in photoexcited iron nanoarrays, *Appl. Phys. Lett.* **110**, 082404 (2017).
- [18] N. Thielemann-Kühn, D. Schick, N. Pontius, C. Trabant, R. Mitzner, K. Holldack, H. Zabel, A. Föhlisch, C. Schüßler-Langeheine, Ultrafast and energy-efficient spin manipulation: Antiferromagnetism beats ferromagnetism, arXiv:1703.03689 (2017).
- [19] G. P. Zhang, W. Hübner, E. Beaurepaire, and J.-Y. Bigot, Laser-induced ultrafast demagnetization: Femtomagnetism, A new frontier?, *Topics Appl. Phys.* **83**, 245 (2002).
- [20] G. P. Zhang and W. Hübner, Laser-induced ultrafast demagnetization in ferromagnetic metal, *Phys. Rev. Lett.* **85**, 3025 (2000).
- [21] T. A. Ostler *et al.*, Ultrafast heating as a sufficient stimulus for magnetization reversal in a ferrimagnet, *Nature Commun.* **3**, 666 (2012).
- [22] A. J. Schellekens and B. Koopmans, Microscopic model for ultrafast magnetization dynamics of multisublattice magnets, *Phys. Rev. B* **87**, 020407 (2013).
- [23] T. D. Cornelissen, R. Cordoba, and B. Koopmans, Microscopic model for all optical switching in ferromagnets, *Appl. Phys. Lett.* **108**, 142405 (2016).
- [24] A. R. Khorsand, M. Savoini, A. Kirilyuk, A. V. Kimel, A. Tsukamoto, A. Itoh, and Th. Rasing, Role of magnetic circular dichroism in all-optical magnetic recording, *Phys. Rev. Lett.* **108**, 127205 (2012).
- [25] V. N. Gridnev, Phenomenological theory for coherent magnon generation through impulsive stimulated Raman scattering, *Phys. Rev. B* **77**, 094426 (2008).
- [26] J. H. Mentink, J. Hellsvik, D. V. Afanasiev, B. A. Ivanov, A. Kirilyuk, A. V. Kimel, O. Eriksson, M. I. Katsnelson, and Th. Rasing, Ultrafast spin dynamics in multisublattice magnets, *Phys. Rev. Lett.* **108**, 057202 (2012).
- [27] M. Berritta, R. Mondal, K. Carva, and P. M. Oppeneer, Ab initio theory of coherent laser-induced magnetization in metals, *Phys. Rev. Lett.* **117**, 137203 (2016); also arX:1604.01188v1 (2016).
- [28] M. I. Kurkin, N. B. Bakulina, and R. V. Pisarev, Transient inverse Faraday effect and ultrafast optical switching of magnetization, *Phys. Rev. B* **78**, 134430 (2008).

- [29] A. Baral and H. C. Schneider, Magnetic switching dynamics due to ultrafast exchange scattering: A model study, *Phys. Rev. B* **91**, 100402(R) (2015).
- [30] G. P. Zhang, Y. H. Bai, and T. F. George, Switching ferromagnetic spins by an ultrafast laser pulse: Emergence of giant optical spin-orbit torque, *EPL* **115**, 57003 (2016).
- [31] G. P. Zhang, T. Latta, Z. Babyak, Y. H. Bai, and T. F. George, All-optical spin switching: A new frontier in femtomagnetism - A short review and a simple theory, *Mod. Phys. Lett. B* **30**, 16300052 (2016).
- [32] X.-J. Chen, Fundamental mechanism for all-optical helicity-dependent switching of magnetization, *Sci. Rep.* **7**, 41294 (2017).
- [33] G. P. Zhang, Y. H. Bai, and T. F. George, A new and simple model for magneto-optics uncovers an unexpected spin switching, *Europhys. Lett.* **112**, 27001 (2015).
- [34] R. Boyd, *Nonlinear Optics*, 3rd Ed. (Academic Press 2008).
- [35] K. A. Chao, J. Spalek, and A. M. Oles, Canonical perturbation expansion of the Hubbard model, *Phys. Rev. B* **18**, 3453 (1978).
- [36] A. J. Ramsay, P. E. Roy, J. A. Haigh, R. M. Otxoa, A. C. Irvine, T. Janda, R. P. Campion, B. L. Gallagher, and J. Wunderlich, Optical spin-transfer-torque-driven domain-wall motion in a ferromagnetic semiconductor, *Phys. Rev. Lett.* **114**, 067202 (2015).
- [37] G. P. Zhang, Microscopic theory of ultrafast spin linear reversal, *J. Phys.: Condens. Mat.* **23**, 206005 (2011).
- [38] G. P. Zhang and T. F. George, Thermal or nonthermal? That is the question for ultrafast spin switching in GdFeCo, *J. Phys.: Condens. Mat.* **25**, 366002 (2013).
- [39] G. Hall and J. M. Watt, *Modern Numerical Methods for Ordinary Differential Equations* (Clarendon Press, Oxford, 1976).
- [40] G. P. Zhang, W. Hübner, G. Lefkidis, Y. Bai, and T. F. George, Paradigm of the time-resolved magneto-optical Kerr effect for femtosecond magnetism, *Nature Phys.* **5**, 499 (2009).
- [41] M. Murakami, Z. Babyak, M. Giocolo, and G. P. Zhang, Quantum mechanical interpretation of the ultrafast all optical spin switching, *J. Phys.: Condens. Matter* **29**, 184002 (2017).
- [42] M. L.M. Laliou, P. L.J. Helgers, and B. Koopmans, Absorption and generation of femtosecond laser-pulse excited spin currents in non-collinear magnetic bilayers, arXiv:1704.03746 (2017).
- [43] T. J. Huisman, R. V. Mikhaylovskiy, J. D. Costa, F. Freimuth, E. Paz, J. Ventura, P. P. Freitas, S. Blügel, Y. Mokrousov, Th. Rasing, and A. V. Kimel, Femtosecond control of

electric currents in metallic ferromagnetic heterostructures, Nat. Nano. **11**, 455 (2016).

TABLE I. Spin change from the initial  $S^i$  to the final  $S^f$  for two mixed spin configurations under laser excitation. The laser pulse duration is 60 fs.  $A_0 = 0.001\text{V}/\text{\AA}$ . All the final spins are collected at time  $t = 661.86$  fs. The numbers in parenthesis are the  $x$ ,  $y$  and  $z$  components. The two columns represent two different spins configurations (see Fig. 1). On the left, the spins in the first layer point along the  $-z$  axis, and the rest are in-plane; On the right, the spins in the first two layers point along the  $-z$  axis, and the rest are in-plane.

Spin $\implies$		$\downarrow\leftarrow\leftarrow\leftarrow\leftarrow$		$\downarrow\downarrow\leftarrow\leftarrow\leftarrow$	
Layer	$S^i(\hbar)$	$S^f(\hbar)$	$S^i(\hbar)$	$S^f(\hbar)$	$S^f(\hbar)$
1	(0,0,-1)	(-0.76, 0.08, -0.20)	(0,0,-1)	(-0.47, -0.04, -0.53)	
2	(-1,0,0)	(-0.77, 0.03, -0.22)	(0,0,-1)	(-0.49, -0.04, -0.52)	
3	(-1,0,0)	(-0.77, -0.05, -0.23)	(-1,0,0)	(-0.52, -0.03, -0.49)	
4	(-1,0,0)	(-0.75, -0.01, -0.23)	(-1,0,0)	(-0.53, -0.04, -0.46)	



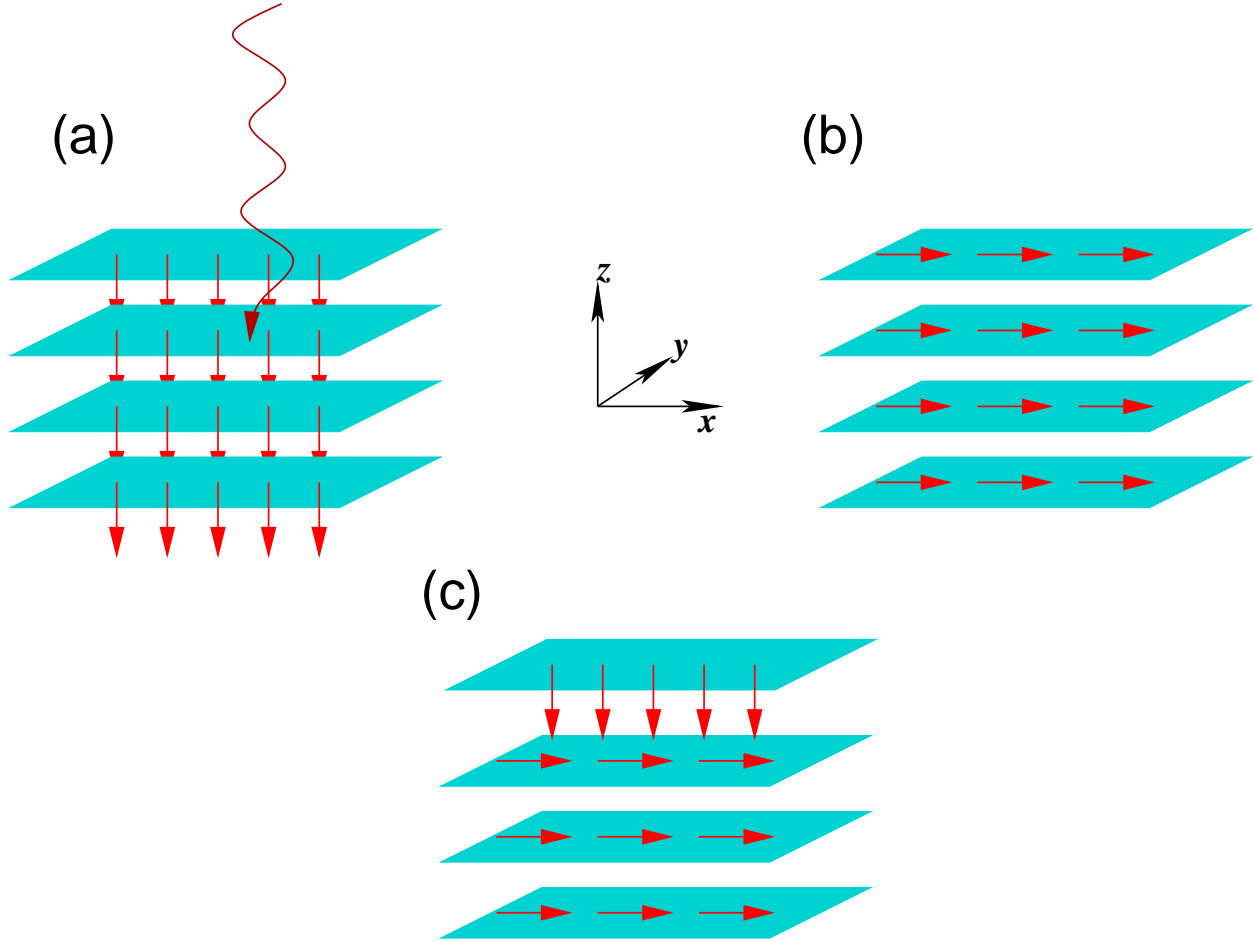


FIG. 1. Three spin configurations used in this paper. Our slab has four monolayers and 41 lattice sites along the  $x$  and  $y$  directions, with the laser light coming from the top with either left-circularly polarized light or right-circularly polarized light. The penetration depth is 40 lattice sites. (a) Perpendicular anisotropy. (b) In-plane anisotropy. (c) Mixed spin orientation. Spins in the first layer are perpendicular, but those in other layers are all in-plane. We also consider a configuration where the first two layers have spin out of plane and the rest in-plane.

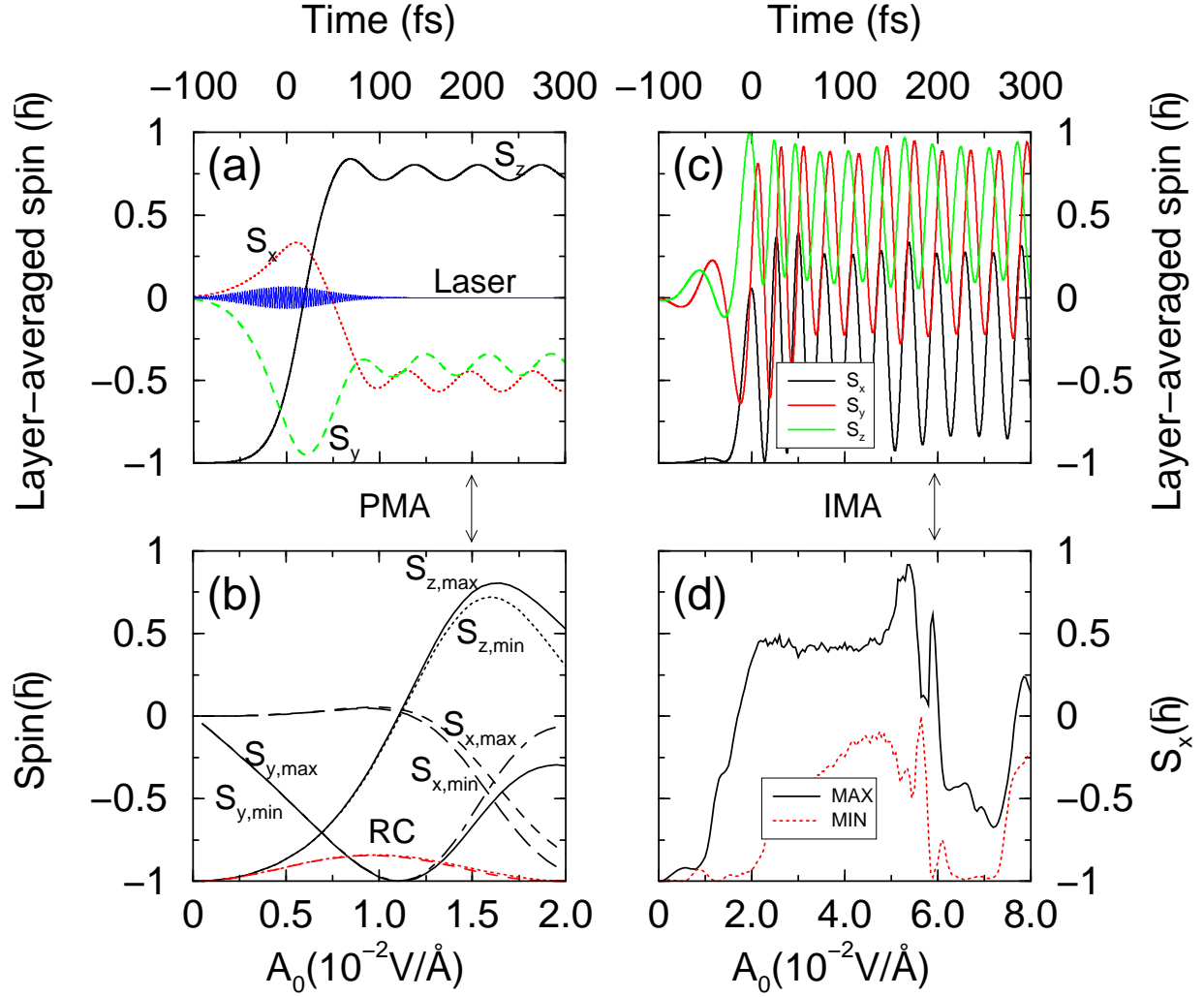


FIG. 2. (a) Layer-averaged spin as a function of time for PMA. Here the spins are from the first layer as other layers are similar. The laser field amplitude is at the optimal value of  $0.0165 \text{ V/\AA}$  (see (b)). The dotted, dashed and solid lines denote the spins along the  $x$ ,  $y$  and  $z$  axes, respectively. Inset: Laser pulse. (b) Laser-field amplitude dependence of the layer-averaged maximum and minimum spins for PMA. The solid and dotted lines are the spin maxima and minima along the  $z$  axis, while rest are along either the  $x$  or  $y$  axis. The helicity-dependence is strong. RC: the results obtained with right-circularly polarized light. (c) Layer-averaged spin as a function of time for IMA with the spin initially along the  $x$  axis. Here the laser field amplitude is chosen to be  $0.02 \text{ V/\AA}$ . (d) Field-amplitude dependence of the layer-averaged spin along the  $x$  axis. The maximum (solid line) and minimum (dotted line) are so different that a huge oscillation is found. Note that the laser field amplitude range is much broader than that in (b) to make sure that we do not miss any possible reversible window. The laser pulse duration is 60 fs.

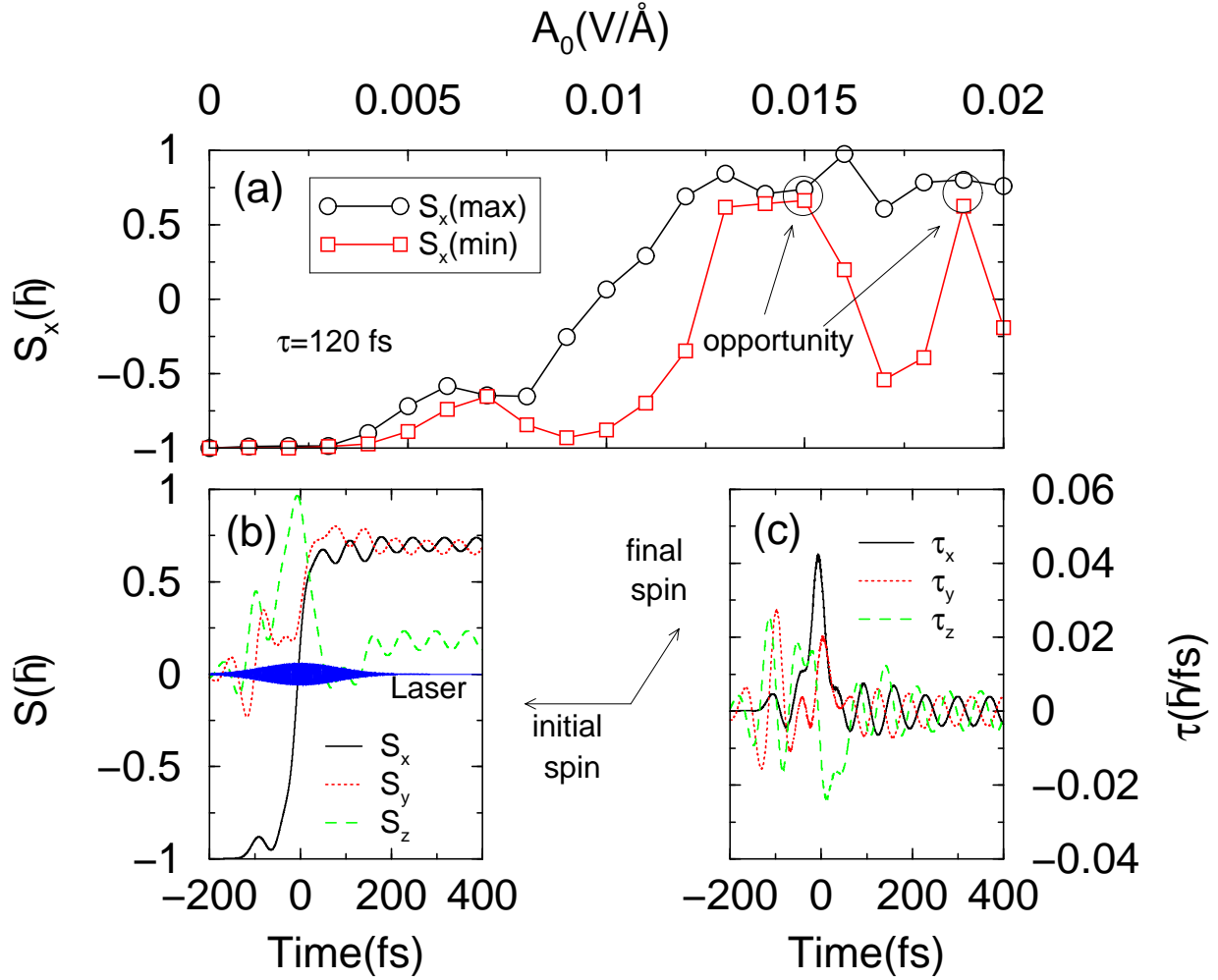


FIG. 3. Longer pulses present an opportunity to reverse the in-plane spins. Here a 120-fs pulse is used. (a) Dependence of the in-plane component of the layer-averaged spin on the laser field amplitude. The empty-circle line denotes the maximum spin, while the empty-box line the minimum. Two circles, the first of which is plotted in (b), highlight two narrow regions where the reversal is possible. Here, the results for the first layer are shown as the rest are similar. (b) Layer-averaged spin change with time. The solid, dotted and dashed lines denote the  $x$ ,  $y$  and  $z$  components, respectively. Inset in (b): Laser pulse. Inset on the right of (b): Depiction of the initial spin and final spin orientations. (c) Spin-orbit torque as a function of time. The key insight is that  $\tau_x$  is larger than  $\tau_y$  and  $\tau_z$ , although it peaks at a latter time and it decreases sharply once the laser pulse ends.

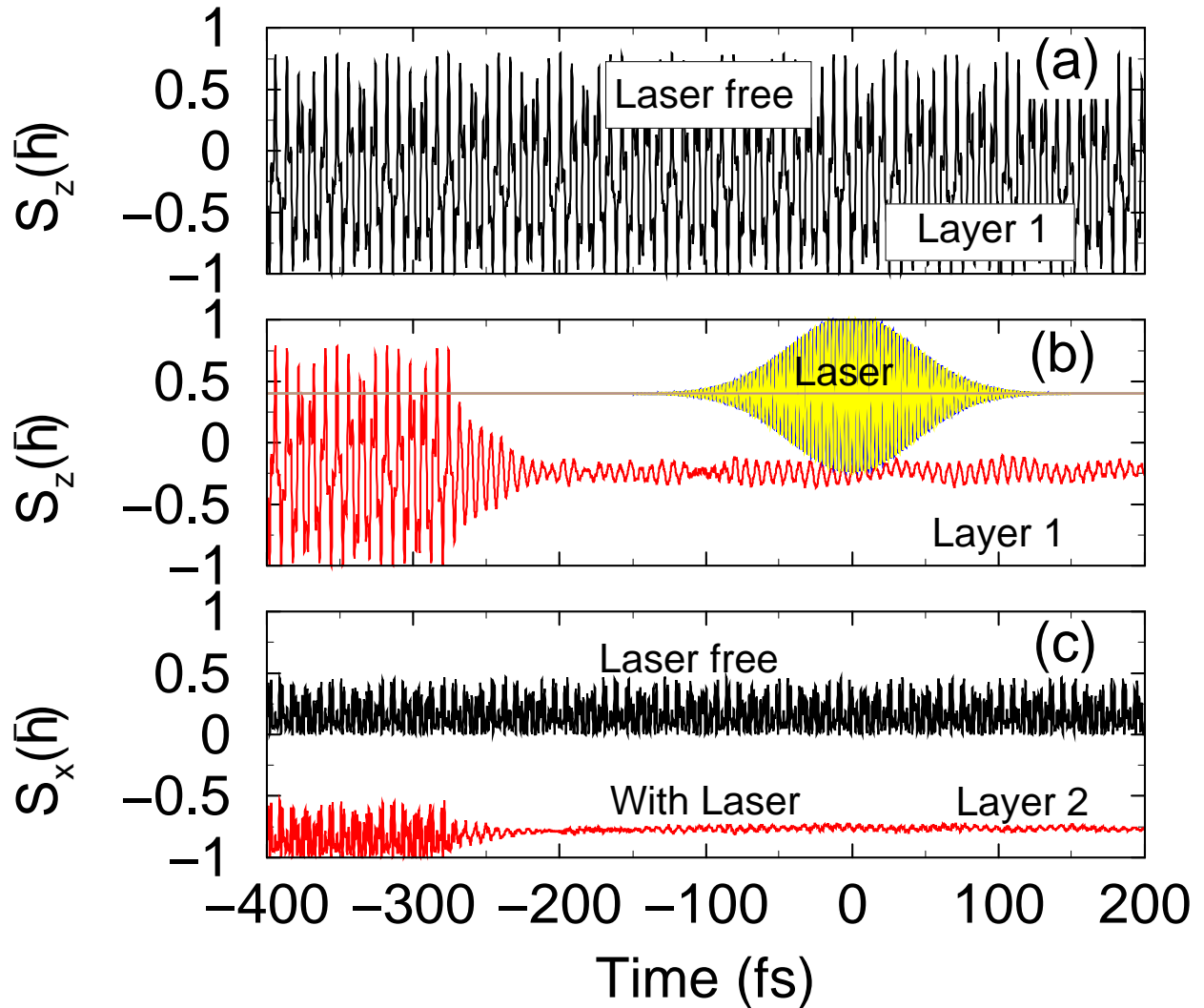


FIG. 4. Laser-induced spin rectification effect in the spin-mixed case. The spin configuration is as follows. The first layer of spin points out of the plane (see 1(c)), while the rest are in-plane. (a) A strong fluctuation of the  $z$  component of the spin in the first layer in the absence of a laser field. (b) The same component as (a) but upon a 60-fs laser excitation. Inset: the laser pulse. The nonzero field already starts around -300 fs. (c) Comparison of the  $x$  component of the spin in layer 2. The spin is also layer-averaged. On the top are the results without a laser field, and on the bottom those with the laser field. The top curve is shifted for clarity. Other layers are similar and not shown.